Evaluation of CORDEX- South Asia regional climate models for heat wave simulations over India

Saumya Singh[a], R.K. Mall[a,*], J. Dadich[a], S. Verma[a], J.V. Singh[b], A. Gupta[c]

[a] *DST-Mahamana Centre of Excellence in Climate Change Research, Institute of Environment and Sustainable Development, Banaras Hindu University, Varanasi, India*
[b] *Ministry of Earth Sciences, New Delhi, India*
[c] *Department of Science and Technology, New Delhi, India*

ABSTRACT

The episodes of heat wave events have strengthened in recent decades causing great concern for human health, agriculture and natural ecosystem. In the present study, Regional Climate Models (RCMs) namely, CCAM and RegCM, from Coordinated Regional Climate Downscaling Experiments (CORDEX) for South Asia (SA) are evaluated for simulating heat waves (March–June) for a long-term period (1971 to 2005) over India in comparison with observations from India Meteorological Department (IMD). The statistical analysis (correlation, RMSE, MAE, ECDF) results reveal differences in RCMs in simulating spatial pattern and trends of maximum temperature before bias correction. Variance scaling bias correction is found to remove bias and improve model simulations in capturing temperature variability. An increase in correlation in daily observations from 0.24 to 0.70 and reduction in RMSE from 8.08 °C to 2.02 °C and MAE from 3.87 °C to 2.43 °C after bias correction is observed between model and observation.

LMDZ4 and GFDL-ESM2M are found to perform best in simulating interannual variability of seasonal mean maximum temperature with an underestimation of −7.74% and −15.41% which improved significantly to around −1.51% and − 0.78%, respectively after bias correction over India. LMDZ4 and GFDL-ESM2M are also best-performing models in significantly reproducing the heat wave frequency and spatial variability in closer proximity with observations over India amongst all models after bias correction. Over NW and western regions, the LMDZ4 and GFDL-ESM2M ensemble models successfully capture the increasing trend of 0.2 events/year and 0.4 events/year accordance to IMD and IITM criteria, respectively. However, the ACCESS1.0, CNRM-CM5 and CCSM4 ensemble experiments overestimated heat waves by ± 40 events in most sub-divisions in India. Over the central Indian regions, the ACCESS 1.0 and CNRM-CM5 model output show a negative trend of −0.2 events/ year and large spatial variability possibly due to model associated uncertainties. Overall the results show an improvement in capturing maximum temperature and heat waves across the regions of Indian sub-continent in the bias-corrected downscaled CORDEX-SA ensemble RCMs than without bias-corrected output. The study suggests a way forward to assess RCMs performance and uncertainty in extreme weather analysis in future projections.

1. Introduction

With the advent of the 21st century, soaring mercury has crossed previously established threshold across the globe. A shift in the global temperature regime at the higher extreme is beyond any doubt or speculation (Alexander et al., 2013; IPCC, 2013). As the global surface temperature observed an increase of 0.85 °C during 1880–2012, the frequency of warmer days and nights has increased since the latter half of the 20th century (IPCC, 2013). These episodes of extreme temperatures have severe consequences in forms of huge mortality due to heat waves, global crop yield anomalies, changing paradigm of species-ecosystem function with rising temperature and mental health risks (Basu, 2009; Mall et al., 2016; García et al., 2018; Obradovich et al., 2018; Singh et al., 2019; Vogel et al., 2019; Mall et al., 2019; Sonkar et al., 2020).

Heat waves are perceived as a manifestation of prolonged extreme temperature, driven and intensified by associated synoptic atmospheric circulations and amplified by regional soil moisture deficit (Quesada et al., 2012; Perkins, 2015; Rohini et al., 2016; Ghatak et al., 2017; Singh et al., 2020). The nature of global heat wave increase resonates

with the Indian subcontinent as recent studies analysing the trend of extreme temperature events over India report an increase in intensity, frequency and duration of heat wave post-1950s (Pai et al., 2013; Rohini et al., 2016; Ratnam et al., 2016; Panda et al., 2017; Mukherjee and Mishra, 2018). The state of this scenario is predicted to persists and aggravate in the future as heat waves are projected to be multi-fold frequent, intense and of longer duration under different emission scenarios (Murari et al., 2015; Perkins-Kirkpatrick and Gibson, 2017; ; Alias et al., 2017; de Perez et al., 2018; Sonkar et al., 2019; Krishnan et al., 2020).

Heat waves have been reported to have killed thousands of people across the world including India. Its seasonal occurrence, high persistence period and concurrent occurrence with drought amplifies the impact many-fold a causing immediate concern (Russo et al., 2015; Ghatak et al., 2017; Sharma and Mujumdar, 2017). Heat waves being a global phenomenon have a severe impact on the local population, to prevent and prepare against heat-related morbidity and mortality it is required to understand the regional characteristics of heat extremes in present as well as in the future. Therefore, a consistent effort to reduce the vulnerability due to heat waves are being made by the scientific community to advance the capacity of characterisation and prediction of heat wave at high-resolution with high accuracy and least uncertainty.

The reliability of future projections of extreme events depends upon the ability of models to simulate the present extremes. IPCC assessment reports have been using and improving the climate models to project future global temperature under different emission scenarios (IPCC, 2013). The Coupled Model Inter-Comparison Project Phase 5 (CMIP5) simulations have been widely used to study the trend of extreme temperature and precipitation for historical and future scenarios (Sillmann et al., 2013; Perkins-Kirkpatrick and Gibson, 2017; Purich et al., 2014; Mall et al., 2018; Almagro et al., 2020). These studies have analysed the climatology, variability and trends of observed climate against those simulated by state-of-the-art global climate models and have found to be reliable for forecasting future variations of the climatic parameters (Alexander and Arblaster, 2017). Mishra et al., 2017b estimated an increase of 3–9 and 16–30 events in frequency of severe heat wave events over India using CESM and CMIP5 simulations for RCP8.5 scenario for 2021–2050 and 2071–2100 from the base period of 1971–2000. Also, future projections of a heat wave over India by using CMIP5 simulations show an increase of 1.5–2.5 heat wave events and increase in the average duration of 12–18 days during 2020–2064 (Rohini et al., 2019).

However, limitations of these models have been reported in capturing orographic and coastal characteristics and also in accommodating local scale dynamic changes (Meehl et al., 2007; Purich et al., 2014). Therefore, an accurate representation of dynamical processes at the regional scale to assess the impact of climate change at a local scale is required. Downscaling provides a way to extrapolate large scale climatic phenomenon to a high-resolution regional-scale to assess the regional impact of climate change (Racherla et al., 2012; Xu et al., 2019). Dynamical and statistical approach has been used to downscale the GCMs. While the former approach uses the physical processes based regional climate models driven by GCM boundary conditions, the latter works on statistical relationships between are local predictands and global predictors (Tang et al., 2016).

The Coordinated Regional Climate Downscaling Experiment (CORDEX) is a regional climate downscaling (RCD) initiative by World Climate Research Program (WCRP) to produce a coordinated framework of regional climate projections for different domains (Giorgi et al., 2009). The rationale behind the CORDEX project stems from the need for coordinated effort of the modeling community to address the limitations in generating comprehensive understanding, evaluation and projection of regional climate information. The primary goal of CORDEX are evaluation of RCD based techniques, uncertainty characterisation and improvement in producing regional climate projections

(Giorgi et al., 2009). To asses the capability of RCMs in representing regional climate characteristics is the first step in CORDEX experimental design. On the basis of evaluation of models reliable future projection can be made at a regional scale.

CORDEX experiments have been widely used for evaluation and projection studies in respective domains serving as baselines of present and future climate change. Jacob et al. (2014) studied the added value to regional climate change information provided by high-resolution EURO-CORDEX RCMs for RCP 4.5 and 8.5 scenarios in comparison to the multi-model ensemble from EU-FP6 ENSEMBLES for the SRES A1B over Europe. The findings indicate that the high-resolution simulations of EURO-CORDEX RCMs increased the regional details and improved climate change projections as compared to ENSEMBLE datasets. Vautard et al. (2013) studied the performance of a large ensemble of RCMs within EURO-CORDEX at two spatial scales of 12 km and 50 km for heat wave persistence and amplitude. The study states an improvement in simulating heat wave events duration (persistence) at a high-resolution while an overestimation for the amplitude by the RCMs.

Lhotka et al. (2017) emphasized on the need of evaluating model performance in simulation of large-scale circulation and land-atmosphere interactions associated with heat waves by RCMs. It was found that the ensemble mean of EURO-CORDEX captures the heat wave extremity index well over Central Europe but individual RCMs overestimated and underestimated the events attributing to inability in simulating associated meteorological phenomenon efficiently High signal to noise ration data is required to study climate change in complex topography regions such as mountains which is difficult to achieve with coarse resolution climate models.

Sanjay et al., 2017 evaluated the mean climatology and changes in seasonal mean temperature and precipitation over Hindu Kush Himalayan region using CORDEX RCMs for near (2036–2065) and far future (2066–2095). Large cold biases were observed in summer and winter seasons in the HKH region against the observation. The bias shown by the RCMs was greater than their driving AOGCMs for temperature. However, both RCMs and AOGCMs overestimated ensemble median total precipitation where RCMs were better than AOGCMs. For far future period under RCP8.5 scenario RCMs showed higher confidence in projecting warming of 5.4 °C during winter than of 4.9 °C in summer and an increase of 22% in summer monsoon precipitation. Studies have evaluated the performance of CORDEX-SA RCMs in simulating Indian summer monsoon variability, extreme precipitation and temperature over India and particular regions but assessment of CORDEX-SA RCMs for heat wave simulation over India is still lacking (Choudhary et al., 2018; Panjwani et al., 2020; Pattnayak et al., 2018; Prajapat et al., 2020).

The objective of the present study is to assess the capability of the high-resolution (50 km) CORDEX-SA RCM outputs in capturing the spatial variability and temporal frequency of heat wave events over India during the historical period (1971–2005) for March–June season. The CORDEX dataset is comprised of downscaled climate scenarios for the South Asia region that are derived from the Atmosphere-Ocean coupled General Circulation Model (AOGCM) runs conducted under the Coupled Model Inter-comparison Project Phase 5 (CMIP5) [Taylor et al. 2012]. The findings of the study are expected to provide a reliable fine-scale model-based projection of heat waves over India in future based on their performance for the historical period. Also, the information provided by this study can be useful in utilizing downscaled RCMs for heat wave forecasting at a regional level based on their regional performance for meteorological subdivisions of India. An inter-model comparison study is undertaken to evaluate the performance of eight bias-corrected ensemble member CORDEX-SA RCMs namely, CCAM and RegCM411 in simulating heat waves over India.

Heat waves are defined based on criteria given by IMD and IITM and the study period extends to heat wave events observed during March–June (1971–2005) over India. Variance scaling method has been used to bias correct the CORDEX-SA RCM outputs to remove any
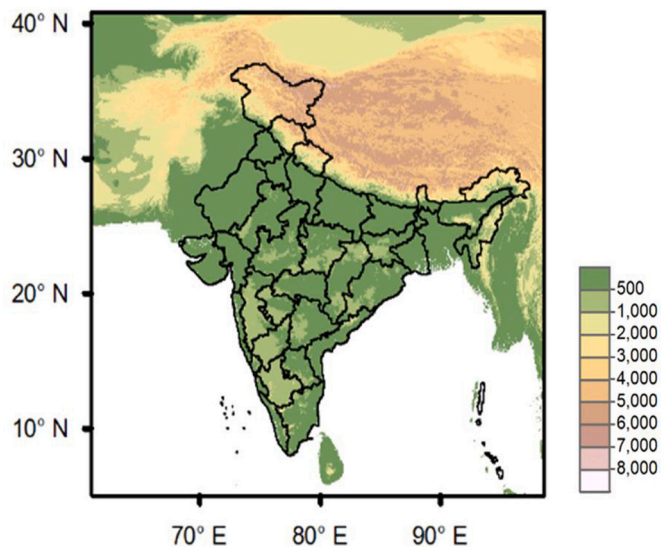
Fig. 1. Topography (in meters) of Indian region and its meteorological sub-divisions considered for the study.

inherent bias and match the climate change signal given by models with that of observed for India and its meteorological subdivisions.Our study provides the first assessment of performances of CORDEX- SA RCMs for heat waves over India which will be useful in future projection studies.

2. Materials and methods

2.1. Study area

The study area extends over Indian region from 8°4′N to 37°6′ N latitude and 68° 7′ E to 97°25′ E longitude in the South Asian region of the CORDEX experiment. The landmass is spread over an area of 3.28 million sq. km accounting for 2.4% of the total world area with a long coastline of 7517 km. The physiography of Indian region exhibits distinct diversity ranging from rugged topography of lofty Himalayan mountain ranges to fertile plains of northern India.

The varied landforms like deserts, Islands, coastal plains and mountainous region etc., has shaped the demographic distribution and livelihood pattern of people in India (Fig. 1).

The climate profile of the country consists of regional variations with tropical climate in the south, sub-humid tropical in the central and temperate climate in the northern Himalayan region. India Meteorological Department (IMD) has categorized the Indian climate in four prominent seasons i) Cold weather season (January–February) ii) Pre-monsoon season (March–May) iii) Southwest monsoon season (June–September) and iv) Post monsoon/Northeast monsoon season (October–December) (Attri and Tyagi, 2010). India receives 75% of its total rainfall during South-West monsoon season with an average annual rainfall of 1190 mm for both the rainy seasons. The rainfall distribution ranges from as low as 50–130 mm in Rajasthan to as high as the world's maximum of around 11,410 mm in Mawsynram. Similarly, the temperature profile of the country shows an extreme distribution ranging from below 0° in the Northern region in winters to above 45 °C during May–June (Attri and Tyagi, 2010). The climatic characteristics and topographical features altogether determine the soil, distribution of flora and fauna and also agricultural practices of the region.

2.2. Data

The study analyses the seasonal heat wave occurrences in hot weather season for March–June during the historical period of 1971–2005 over India at each grid level of 0.5° × 0.5° resolution using

model simulations and observation datasets. Daily gridded maximum surface air temperature (T_{max}) developed by Srivastava et al. (2009) was obtained from the India IMD at the resolution of 50 km for the study period. The regional climate simulations for India was obtained from CORDEX South Asia experiments which extend over the South Asian region from 19.25°E–116.25°E and 15.75°S–45.75°N at a resolution of 0.5° (~50 km). The data represents eight CORDEX-SA experiments in which the eight experiment datasets comprise of an ensemble of eight dynamically downscaled projections using a high-resolution regional climate model. Conformal-Cubic Atmospheric Model (CCAM) driven from six different Global Climate Models (GCMs) namely AC-CESS 1.0, CCSM4, GFDL-CM3, CNRM-CM5, MPI-ESM-LR and NorESM-1 M (Table1.).

The other two experiments use RegCM4.1.1 regional climate model contributed by the Center for Climate Change Research, Indian Institute of Tropical Meteorology (CCCR-IITM) forced by boundary conditions from LMDZ4 and GFDL-ESM2M global climate model. The RCM dataset obtained from CCCR-IITM was daily 2 m near-surface maximum temperature at a spatial resolution of 0.5° × 0.5° latitude-longitude grid which corresponds to a horizontal resolution of ~50 km for March–June during the historical period of 1971–2005 for 1099 grids over India. In the study, the downscaled RCM output dataset (raw) were bias-corrected using variance scaling method (bias-corrected output). This bias-corrected dataset was used for model performance evaluation. The specifications of the ensemble members of CCAM and RegCM4.1.1 RCMs of CORDEX-SA experiment is given in Table 1.

2.3. Heat wave indices

While defining heat wave it is indispensable to consider different aspects that are crucial to measuring the degree of impact it will have on human health, wildlife, agriculture, infrastructure and economy. Over the course of extensive research on understanding the nature of the threat posed by prevailing extreme temperature, the scientific communities (Expert Team on Climate Change Detection and Indices (ET-CCDI)) and researchers have adopted various indices to quantify the degree of severity associated with heat wave (Karl et al., 1999; Peterson et al., 2001; Perkins and Alexander, 2012). Studies in the past have explored from simple metrics based on thresholds and percentiles to relatively complex indices consisting of departures from long term normal along with percentiles based on varying moving windows.

A recent study attempts to understand the temporally compound structure of heat waves identified as the occurrence of intermittent short breaks of maximum cooler number of days between minimum consecutive hot days to mark the beginning and end of heat wave event (Baldwin et al., 2019). Indices for identifying heat wave are not restricted to measuring only day time temperature as the high nighttime temperature and reduced diurnal temperature exacerbate the impact in absence of discharge of daytime heat (Gosling et al., 2009). A period of three days has been widely used as a measure of persistent heat wave imposing a health hazard. Mukherjee and Mishra (2018) considering the impact of persisting high night time temperature consecutive 3 days moving average for daily maximum and minimum temperature to compute concurrent hot day and hot night (CHDHN)as an index of heat wave.

A detailed analysis of the impact of temperature must account the nature of physiography of the region, surrounding environmental condition particularly vegetation, socio-economic conditions and degree of exposure of the population. Hence, the topography and environment have a profound impact on temperature variation and so the indices vary regionally. In the present study, we have used two different criteria given by IMD (IMD, 2018) and IITM (Mandal et al., 2019) (Fig. 2.) to declare heat wave events and also to compare the relative performance of models in simulating heat waves through both the criteria.

The IMD criteria should be met for at least two stations in a

Table 1
Details of the CMIP5 models used for the analysis (Source: http://cccr.tropmet.res.in).

CORDEX South Asia RCM Experiment	Name used	RCM Description	Contributing CORDEX Modeling Center	Driving CMIP5 AOGCM
CCAM (ACCESS)	ACCESS 1.0	Commonwealth Scientific and Industrial Research Organisation (CSIRO), Conformal-Cubic Atmospheric Model (CCAM; McGregor and Dix, 2001)	CSIRO Marine and Atmospheric Research, Melbourne, Australia	ACCESS1.0 (Collier and Uhe, 2012; Bi et al., 2013)
CCAM (CCSM4)	CCSM4			Community Climate System Model 4 (CCSM4; Gent et al., 2011)
CCAM (GFDL)	GFDL-CM3			Geophysical Fluid Dynamics Labora- tory Climate Model version 3 (GFDL-CM3; Griffies et al., 2011)
CCAM (CNRM)	CNRM-CM5			CNRM-CM5 (Voldoire et al., 2013)
CCAM (MPI)	MPI-ESM-LR			Max Planck Institute for Meteorology, Germany, Earth System Model (MPI- ESM-LR; Giorgetta et al., 2013)
CCAM (BCCR)	NorESM1-M			Norwegian Earth System Model(NorESM1-M; Bentsen et al., 2013)
RegCM (LMDZ4)	LMDZ4	The Abdus Salam International Centre for Theoretical Physics (ICTP) Regional Climatic Model version 4.1.1 (RegCM4; Giorgi et al., 2012)	CCCR, IITM, India	LMDZ4 (Global variable grid atmospheric model forced with bias-corrected SST; Sabin et al., 2013))
RegCM (GFDL-ESM2M)	GFDL-ESM2M			Geophysical Fluid Dynamics Labora- tory, USA, Earth System Model (GFDL-ESM2M-LR; Dunne et al., 2012)

meteorological sub-division for consecutive days and heat wave will be declared on the second day while each day fulfilling IITM criteria is declared as a heat wave. Heat waves in hilly, plains and coastal region of India have been declared according to the different thresholds mentioned in IMD criteria.

2.4. Bias correction

As climate models simulate the interaction of climatic variables of the complex climate system, it is indispensable to account the uncertainty associated with model simulation for any analysis. Regional climate model simulations are associated with certain bias owing to the model systematic error and inaccurate physical parameterizations (Christensen et al., 2008;). To improve the model simulations for climate change impact assessment studies several simple to sophisticated bias correction approaches have been developed such as linear scaling, function transfer and distribution mapping (Schmidli et al., 2006; Themeßl et al., 2012; Chen et al., 2013).

Typical biases in RCMs are associated with simulations of mean and variability of the climate variables which are corrected using factors based on differences in mean and ratio of variances of raw model simulations and observed data for a reference period using linear and non-linear equations. These methods aim to improve day to day variability of the climate variables and fitting model simulations to the observations for the time series with little emphasis on extreme values. In the case of hydrological extremes, distribution mapping methods which require the construction of transfer functions to correct bias for present and future projections have been found to perform well (Teutschbein and Seibert, 2012). To assess the performance of bias correction in simulating extreme temperature both at lower and higher ends kernel density distribution for daily maximum temperature has been estimated in the present study.

Variance scaling method given by Chen et al. (2011a, 2011b) was adopted for bias correction of the historical ensemble simulations (1971–2005) against observed data from IMD for effective heat wave simulation. Variance scaling method adjusts both mean and variance associated bias in RCM simulations and so are better than mean adjusting approaches and have been found to perform well for bias correction of model simulations (Teutschbein and Seibert, 2012; Fang et al., 2015; Luo et al., 2018). Teutschbein and Seibert (2012) have simplified the variance scaling equations given by Chen et al. (2011a, 2011b) in the following steps:

In the first step, linear scaling is performed for correcting daily maximum temperature ($T_{contr}^{*1}(d)$) by adding the difference between mean monthly temperature of observed (IMD) and RCM datasets $\mu_m(T_{obs}(d)) - \mu_m(T_{contr}(d))$ to RCM daily maximum temperature T_{contr} for the period 1971–2005. The monthly mean maximum temperature is obtained for each of the month (March–June) for the reference period of 1971–2000 for both observed and model output.

$$T_{contr}^{*1}(d) = T_{contr}(d) + \mu_m(T_{obs}(d)) - \mu_m(T_{contr}(d) \tag{1}$$

In the next step before variance scaling the mean corrected daily model data are shifted to zero mean and standard deviation of one on a monthly basis using the following equation:

$$T_{contr}^{*2}(d) = T_{contr}^{*1}(d) - \mu_m(T_{contr}^{*1}(d)) \tag{2}$$

Further, the variance of model simulations from step 2 ($T_{contr}^{*2}(d)$) is scaled by the ratio of the monthly standard deviation of observed data $\sigma_m(T_{obs}(d))$ to the monthly standard deviation of model data $\sigma_m(T_{contr}^{*2}(d))$ using the following equation:

$$T_{contr}^{*3}(d) = T_{contr}^{*2}(d) \times \left| \frac{\sigma_m(T_{obs}(d))}{\sigma_m(T_{contr}^{*2}(d))} \right| \tag{3}$$

In the final step, the bias-corrected daily RCM temperature data are obtained by adding corrected mean to the variance scaled daily
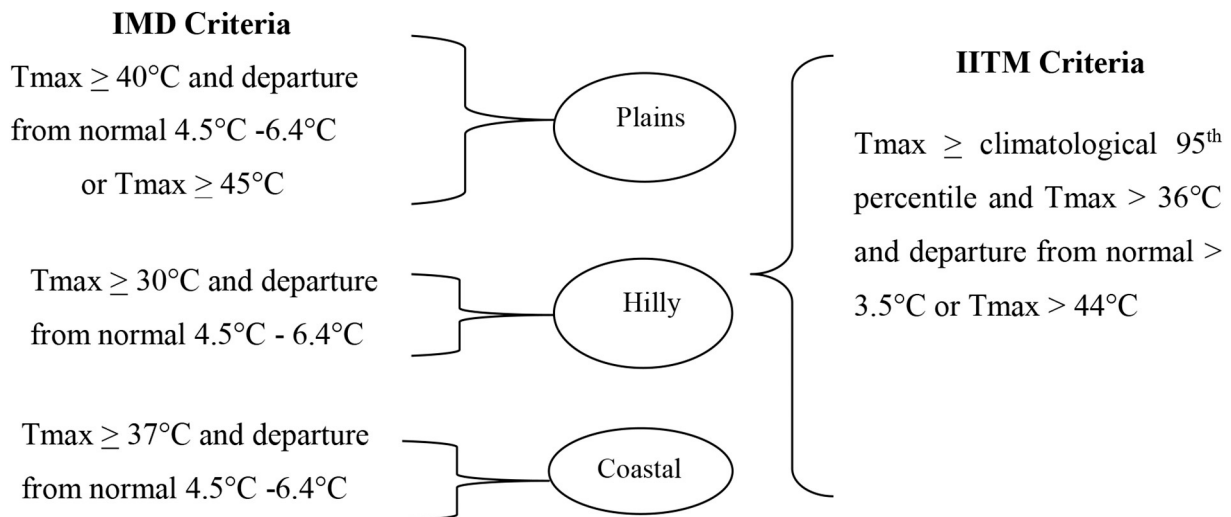
IMD Criteria

Tmax ≥ 40°C and departure

from normal 4.5°C -6.4°C

or Tmax ≥ 45°C

Plains

IITM Criteria

Tmax ≥ climatological 95th

percentile and Tmax > 36°C

and departure from normal >

3.5°C or Tmax > 44°C

Tmax ≥ 30°C and departure

from normal 4.5°C - 6.4°C

Hilly

Tmax ≥ 37°C and departure

from normal 4.5°C -6.4°C

Coastal

Fig. 2. IMD and IITM Criteria for Heat Wave Events.

maximum temperature for the entire study period of 1971–2005 using the following equation.

$$T^*_{contr}(d) = T^{*3}_{contr}(d) + \mu_m(T^{*1}_{contr}(d)) \qquad (4)$$

where $_{contr}$ is RCM-simulated 1971–2000, d is daily, $_{obs}$ is observed maximum temperature, $-\sigma_m$ is the monthly standard deviation, μ_m is monthly mean, * is final bias-corrected *1,2,3 is the intermediate bias-corrected model. The mean and standard deviation of the RCMs were found to be same as that of the observed which ensures that the bias correction is performed correctly. Fig. S1 & S2 and Table S2 show that after bias correction the RCM mean maximum temperature for Mar-Jun (1971–2005) and the standard deviation is same as that of observed.

2.5. Statistical analysis

To assess the performance of RCMs in simulating seasonal mean maximum temperature after bias correction Empirical Cumulative Distribution Function (ECDF) was constructed. ECDF shows if the bias-corrected model simulations are able to reproduce the data as observed or the bias exists in the form of over or underestimation in the density distribution of the data. These assessments help in selecting the best fit model for impact studies (Russo et al., 2014; Russo et al., 2015; Wang et al., 2016). Kernel Density Estimate (KDE), a non-parametric and empirical method of probability density distribution is applied to study and compare the distribution of daily maximum temperature of the raw and bias-corrected model datasets with observed data over each grid of the meteorological subdivisions of India (O'Brien et al., 2016).

In the study, we use different statistical metrics which provide an objective measure to assess the relative performance of bias-corrected RCM outputs in simulating the maximum surface air temperature over India. To measure this relative improvement we have estimated the Root Mean Square Error (RMSE), Mean Absolute Error (MAE) and Willmot's index of agreement (d) which is the ratio of the mean square error and the potential error (PE) multiplied by N (no. of observation) and then subtracted from one which is a standardized measure of the degree of model prediction error and varies between 0 and 1. A value of 1 indicates a perfect match, and 0 indicates no agreement at all (Willmott, 1981). These metrics measure the overall bias and degree of similarity between raw model dataset and bias-corrected data with observations (Gleckler et al., 2008).

Taylor diagram has been widely used to evaluate the performance of RCM simulations against observation. It provides an easily interpretable graphical statistical summary of different metrics indicating the degree to which the model and observed patterns match each other (Taylor,

2001; Gleckler et al., 2008; IPCC, 2013; Miao et al., 2014; Harrison et al., 2015; Gupta et al., 2020). In the diagram, while the root mean square error measures centered mean differences between the two fields, standard deviation quantifies the variance and pattern correlation indicate the similarity between raw model, bias-corrected model and observed data (Taylor, 2001; Gleckler et al., 2008).

To estimate the suitability of the individual models for studying heat wave characteristics over India long term linear trends at the significance level of 90% were estimated to determine any possible long- term increasing or decreasing spatio-temporal trend in the occurrence heat waves as simulated by ensemble members against observed (Yao et al., 2013; Rohini et al., 2019)

3. Result & discussions

3.1. Temporal variability and probability density distribution

The CORDEX-SA raw and bias-corrected output has been compared to that of IMD observations to assess their ability in simulating maximum temperature over India. The study evaluates the model performance using ECDF, RMSE, MAE, index of agreement and Taylor diagram using the seasonal mean of daily maximum temperature during March–June (1971–2005) of all the grids over India. Fig. 3. shows the ECDF of the seasonal mean of daily maximum temperature from all eight ensemble RCM outputs, bias-corrected model output and IMD observed maximum temperature. The distribution shows a clear difference between maximum temperature simulated by both the ensembles before bias correction. The mean maximum temperature simulated by GFDL-ESM2M (31.84 °C) and LMDZ4 (34.73 °C) of RegCM4.1.1 ensemble is underestimated by − 15.41% and − 7.74% respectively against the observed (37.64 °C).

This underestimation is reduced to −0.78% and − 1.51% after bias correction of the model data. The CCAM ensemble members, overestimate the mean maximum temperature 41.92 °C (CCSM4), 41.26 °C (MPI-ESM-LR) with that of observed 11.37% and 9.62% which reduces to 4.28% and 3.05% after bias correction. A significant improvement is observed after variance scaling, as indicated in Fig. 3 where each of the bias-corrected model output distribution (dashed lines) followed the observed (red line) distribution of maximum temperature closely. MPI-ESM-LR simulates the minima and maxima as 23.65 and 38.79 °C closest to the observed with least overestimation of 0.80% and 3.06% in CCAM ensemble while GFDL-ESM2M performs the best after bias correction in RegCM4.1.1 ensemble by exhibiting the minima and maxima of 24.50 °C and 37.35 °C with an overestimation of 4.44% and
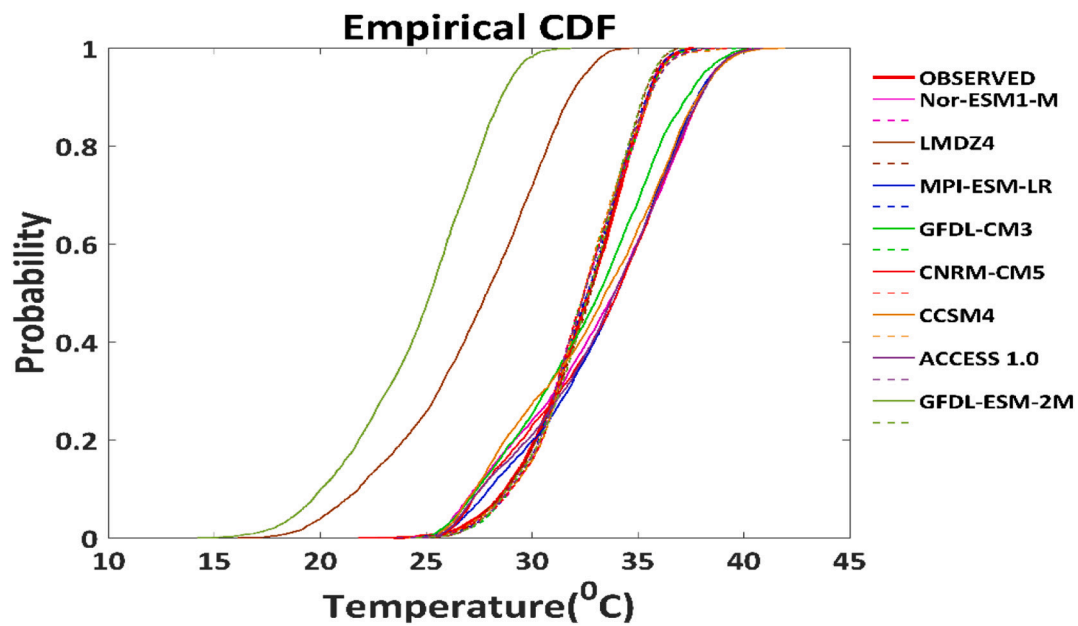
Fig. 3. Empirical Cumulative Density Function of CORDEX- RCMs before and after bias correction.
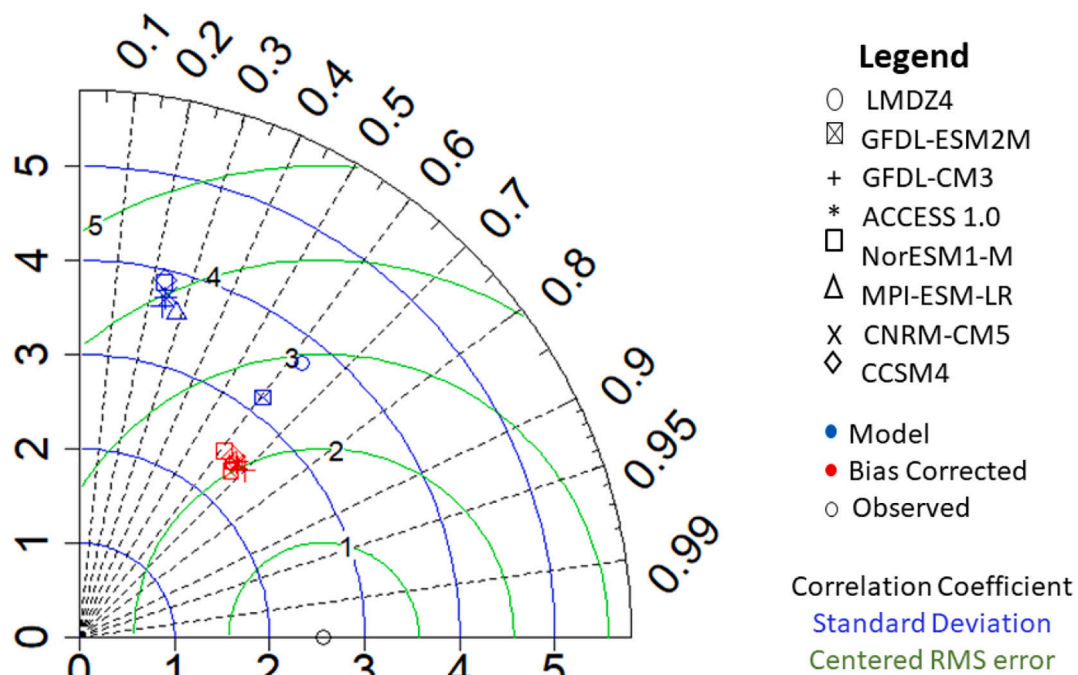

Fig. 4. Taylor Diagram showing model performance of CORDEX- RCMs before and after bias correction.

underestimation of −0.78% respectively. Taylor diagram (Fig. 4) shows the large intermodel spread in RMSE, standard deviation and correlation coefficient between CCAM and RegCM411 ensemble dataset with the observed which reduces after bias correction. After bias correction all of the RCM simulations approximate the observation to a great extent as a decrease from 3.87 °C to 2.43 °C in deviation and centred root mean square error of 8.08 °C to 2.02 °C and increase in correlation coefficient from 0.23 to 0.70 is observed.

3.2. Performance statistic metric and bias estimation

The statistical measure of fidelity between model simulations and observation is estimated using MAE, RMSE and d as given in Table 2. The absolute measure of the models shows GFDL-CM3 have least RMSE

Table 2

Root mean square error (RMSE), mean absolute error (MAE) and Index of agreement (d) of raw (mod) and bias-corrected (var) model data datasets.

Model	RMSE (mod) (°C)	RMSE (var) (°C)	MAE (mod) (°C)	MAE (var) (°C)	D (mod)	d (var)	R (mod)	r (var)
CNRM-CM5	4.19	2.06	3.55	1.61	0.52	0.81	0.25	0.67
CCSM4	4.19	2.13	3.55	1.66	0.51	0.80	0.23	0.65
LMDZ4	5.83	2.08	5.12	1.67	0.52	0.81	0.63	0.66
NorESM1-M	4.21	2.23	3.57	1.73	0.51	0.78	0.23	0.61
GFDL-CM3	3.92	1.95	3.28	1.51	0.52	0.83	0.24	0.70
MPI-ESM-LR	3.93	2.07	3.31	1.64	0.51	0.78	0.28	0.66
ACCESS 1.0	4.09	2.07	3.49	1.62	0.51	0.81	0.24	0.66
GFDL-ESM2M	8.08	2.02	7.50	1.61	0.40	0.81	0.60	0.68

Table 3
Relative measure of performance of bias correction for CORDEX-RCMs as ratio of model to bias corrected (var) data for RMSE, Index of Agreement (d), and Mean Absolute Error (MAE).

Model	RMSE (mod) / RMSE (var)	MAE (mod) / MAE (var)	d (var) / d (mod)
CNRM-CM5	2.03	2.20	1.56
CCSM4	1.97	2.14	1.57
LMDZ4	2.80	3.07	1.56
NorESM1-M	1.89	2.06	1.53
GFDL-CM3	2.01	2.17	1.60
MPI-ESM-LR	1.90	2.02	1.53
ACCESS 1.0	1.98	2.15	1.59
GFDL-ESM2M	4	4.76	2.03

of 1.95 °C followed by GFDL-ESM2M (2.02 °C) after bias correction which had the highest RMSE of 8.08 °C before bias correction. Similarly, in the metric of MAE, GFDL-CM3 have least MAE of 1.5 °C, followed by GFDL-ESM2M (1.61 °C) and CNRM-CM5 (1.61 °C).

Amongst all of the ensemble members GFDL-CM3 has the highest index of agreement (0.83) with the observed maximum temperature while NorESM1-M and MPI-ESM-LR have the least index of agreement (0.78). These measures indicate GFDL-CM3 perform significantly better amongst eight ensembles and NorESM1-M has the least score in simulating daily mean maximum temperature over India.

To assess the relative improvement of the models after bias correction a ratio-based assessment of raw model output to bias-corrected output (var) for each of the performance metric is computed as given in Table 3. shows GFDL-ESM2M and LMDZ4 observe around 2–4 times decrease in MAE and a similar increase in agreement with the observation.

3.3. Kernel density estimation for meteorological sub-divisions

Fig. S3. shows KDE plots of the daily maximum temperature of the three fields (i.e., raw, bias- corrected and observed) for March–June (1971–2005) for each of the meteorological subdivisions except for Andaman Nicobar and Lakshadweep island. The distribution helps to identify the most suitable model for studying extreme temperature for each of the meteorological subdivision. The distribution shows that each of the model outputs can simulate maximum temperature similar to that of observed after bias-correction. A common observation in the raw dataset for each of the subdivision shows that the CCAM ensemble member models overestimate the maxima in most of the subdivisions. The overestimation in °C ranges from 6 °C to 11 °C and more such as it simulates as high as 56.03 °C in Punjab (NorESM1-M) and 55.57 °C for West Rajasthan (CCSM4). Whereas RegCM411 ensemble member underestimate the maxima and minima in subdivisions which are observed over a range of −37.44 °C to −0.72 °C for J&K (LMDZ4) and Kerala (GFDL-ESM2M) in minima and respectively −9.18 °C and to −0.12 °C for Himachal Pradesh (LMDZ4) and Coastal Karnataka (GFDL-ESM2M) for maxima.

While GFDL-ESM2M and LMDZ4 have been found to stimulate both temperature range and probability density in agreement with observations over most of the subdivisions after bias-correction as given in Fig. 5 which shows the models performing best and worst before (solid line) and after bias correction (dotted line) with reference to the observed. There has been a significant improvement in simulations after bias correction for hilly subdivisions such as Himachal Pradesh, Jammu and Kashmir where both the ensemble member dataset (raw) failed to capture the temperature variations showing both cold and warm bias. For mountainous areas, it is important to understand the elevation difference between observed and simulated. As the elevation in the models is smoothed models overestimate temperatures for hilly stations. In Kashmir perhaps the station is in a valley surrounded by high

mountains causing a negative bias. The density estimates for East and West Madhya Pradesh found CCAM ensemble members to underestimate the peak while GFDL-ESM2M performs the best.

After bias correction, ACCESS 1.0, CCSM4, CNRM-CM5 performed better as the bias reduced to 0.13%, − 1.85% and 0.75% in maxima and 19.13%, 8.75%, −7.85% in minima of temperature respectively in case of Haryana, Delhi and Chandigarh subdivision. Variance scaling does not perform well for Chhattisgarh, East MP, Gangetic WB, Jharkhand and Orissa as CCAM ensemble models underestimate the lower maximum temperature in the range of −12.89% to −33.85%. Where ACCESS1.0 and CNRM-CM5 show the highest negative bias of −38.08% and − 33.85%. while RegCM4 show relatively lower bias of 0.67% to 17.5% in these subdivisions. For Madhya Maharashtra, Rayalaseema, West Uttar Pradesh, Tamil Nadu and Puducherry both ensemble members follow the observed temperature reasonably well after bias correction.

As the majority of the subdivisions can reproduce the daily maximum temperatures over the subdivisions, the bias-corrected model output can be used to evaluate the performance of models in heat wave estimation. Nayak et al. (2019) found that RegCM4 performs reasonably well in simulating temperature over India particularly in the northwestern region where extreme temperatures are observed. Our results correlate well with a recent study evaluating the performance of GCMs which found GFDL-ESM2M better in simulating extreme temperature over India (Panjwani et al., 2020).

To understand the pattern of temporal variations shown by raw and bias corrected model output with reference to observed a time series of annual mean maximum temperature (Mar-Jun) during the period 1971–2005 is constructed (Fig. 6). Assam & Meghalaya, East Madhya Pradesh, Gujarat, Jammu and Kashmir, Odisha, Tamil Nadu, Vidarbha and West Rajasthan meteorological subdivisions which represent hilly, plain and coastal areas of northern, eastern, western and southern region of the country are selected for the see the temporal variations. A common observation for all the models shows that Both raw model output (raw) and bias corrected (var) model output show same pattern of interannual variability There is no effect of bias correction on temporal pattern of the output but the magnitude of difference in annual means is reduced remarkably after bias correction.

It was observed that CNRM-CM5, GFDL-CM3, GFDL-ESM2M MPI-ESM-LR and LMDZ4 are more consistent in following the observed annual cycle than ACCESS 1.0, CCSM4 and NorESM1-M in most of the sub-divisions (Figure). None of the models have followed the observed temporal characteristics exactly but show some consistency with the reference. For the coastal regions of Odisha and Gujarat CNRM-CM5, GFDL-CM3, MPI-ESM-LR and GFDL-ESM2M follow the observed pattern for longer duration. The timeseries for Vidarbha which is a heat wave prone region shows GFDL-CM3 and MPI-ESM-LR are found to simulate the observation well particularly after late 1980s period. While CCSM4, CNRM-CM5, LMDZ4 and GFDL-ESM2M capture the years with steep decline or increase in temperature for West Rajasthan.

In the hilly region of Jammu and Kashmir where large cold bias is shown by both the ensembles (CCAM and RegCM4), CCSM4 and MPI-ESM-LR performed best followed by GFDL-ESM-2M and LMDZ4. GFDL-CM3 followed by GFDL-ESM-2M and LMDZ4 are better in Eastern Madhya Pradesh. In north eastern part of the country (Assam & Meghalaya) GFDL-CM3, CNRM-CM5 simulate the temporal pattern very well with the observation followed by GFDL-ESM2M and in the southern region (Tamil Nadu & Pondicherry) CNRM-CM5, LMDZ4 and GFDL-ESM2M are found better.

3.4. Simulation of heat wave events using IMD and IITM criteria

3.4.1. IMD criteria

The ability to simulate heat waves by bias-corrected CORDEX-RCMs is assessed by comparing the model simulations with observed heat wave events calculated using IMD criteria for March–June during the
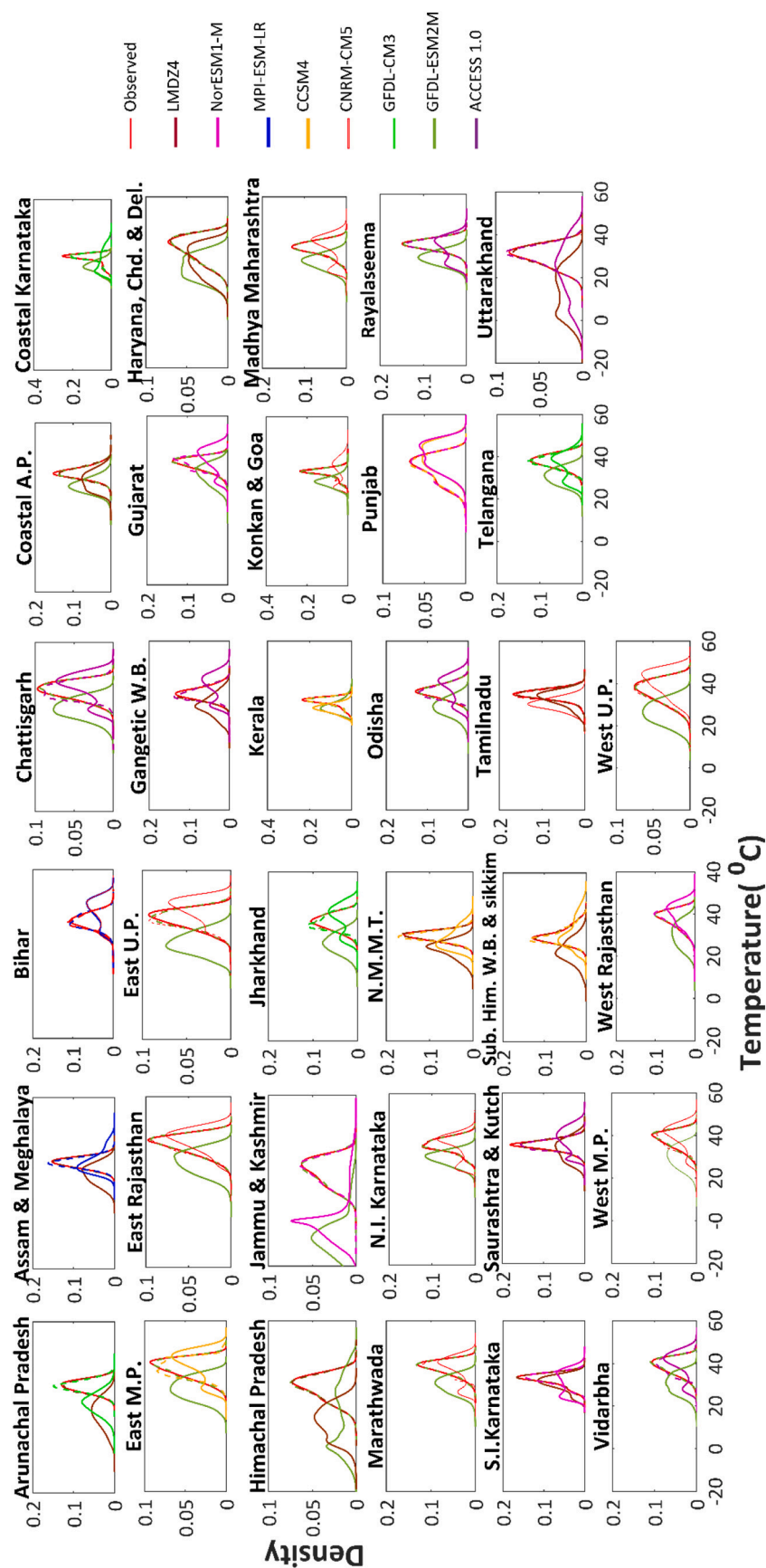
Fig. 5. Kernel Density Estimate of observed and best andworst performing CORDEX- RCMs for March–June during 1971–2005 over meteorological subdivisions of India (raw model and bias corrected output are shown by solid and dotted line respectively in the figure).
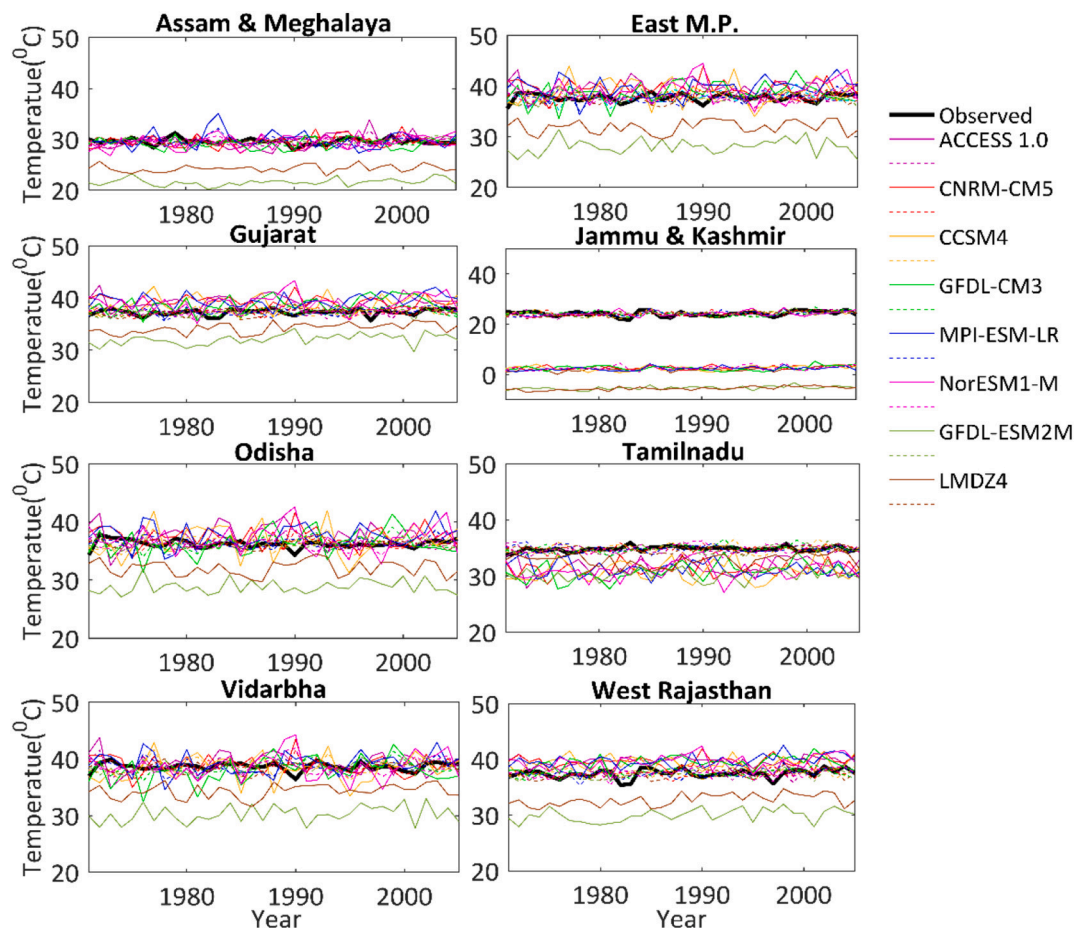
Fig. 6. Timeseries of seasonal mean maximum temperature (Mar-Jun) during 1971–2005 for observed, raw (solid line) and bias-corrected (dotted line) CORDEX-RCM output over India.

period 1971–2005 (Fig. 7 a). The analysis shows that heat wave events are observed over most of the region of India except for SW region constituting of parts of Karnataka, Kerela, Madhya Maharashtra.

The frequency of heat wave events for the season was maximum in central (> 140 events), northwestern (~110 events) and south-central region (~90 events) which cover East MP, West MP, East UP, West UP, East Rajasthan, West Rajasthan, Himachal Pradesh and Vidarbha meteorological subdivision. Both CCAM and RegCM4 members simulate the highest frequency of heat waves over these regions as observed. However, the occurrence varies for each of the models.

LMDZ4, GFDL-ESM2M and MPI-ESM-LR have been found to simulate cumulative heat wave frequency in the range of 90–130, 100–150 and 100–130 events similar to that of observed (90–150 events) in highest heat wave recording regions (East and West MP). GFDL-CM3 (100–110 events) and CNRM-CM5 (> 120 events) also resemble close to the observations while CCSM4 and ACCESS 1.0 overestimate the events recording 140–170 and 140–190 events in the above region. An overestimation in spatial variability is shown by MPI-ESM-LR and NorESM-1 M for parts of East and West MP. These two models report > 120 heat wave events in those parts where < 90 events are recorded in observation.

GFDL-ESM2M recorded 90–100 and 100–110 heat wave events for West and East Rajasthan events similar to the observed (90–100 and 100–110 heat wave events. Moreover, LMDZ4 with < 90 events and MPI-ESM-LR with < 100 events perform fairly well while CCSM4 and ACCESS 1.0 overestimate for both the subdivisions with 100–140 events. An underestimation of heat waves is observed over West Rajasthan by GFDL-CM3 (< 60 events) and NorESM-1 M (< 80 events). In West and East UP highest heat wave frequency of 90–120 events is

observed which is best simulated by LMDZ4 (80–120 events) and GFDL-CM3 (80–110 events).

For Vidarbha region which is extremely vulnerable to the impact of heat wave events GFDL-ESM2M and MPI-ESM-LR record a maximum of 80–100 events as observed providing better results. In case of the hilly region in Himachal Pradesh and Jammu and Kashmir where large bias was observed before bias correction, GFDL-ESM2M is found to reproduce the events better. For the southern coastal region (Kerala and Tamil Nadu and Puducherry) it is observed that CCAM ensemble models record an occurrence of heat wave events whereas LMDZ4 and GFDL-ESM2M ensemble for RegCM4 do not show heat waves in the region similar to the observed. This indicates that RegCM4 models are comparatively better at capturing associated atmospheric circulations in the coastal region. High-resolution.

The boxplot in Fig. 8 shows the comparison of heat wave frequency as calculated from CORDEX RCMs data in comparison to IMD datasets for 1971–2005 where LMDZ4 has found to be most similar in lower quartile (301.5), median (704) upper quartile (1333.5) and as observed (IMD) (269.5, 649 and 1332).

3.4.2. IITM criteria
IITM criteria has been used for forecasting and prediction of heat wave events over India in a recent study by Mandal et al. (2019). It is a percentile-based criterion and estimates each day for heat wave according to the threshold, unlike IMD criteria which accounts for consecutive two days for declaring heat waves. The North Western, Central and South-Central region of the country observe the highest frequency of heat wave events similar to as recorded using IMD criteria. This shows that both the criteria fulfil the conditions for defining heat waves
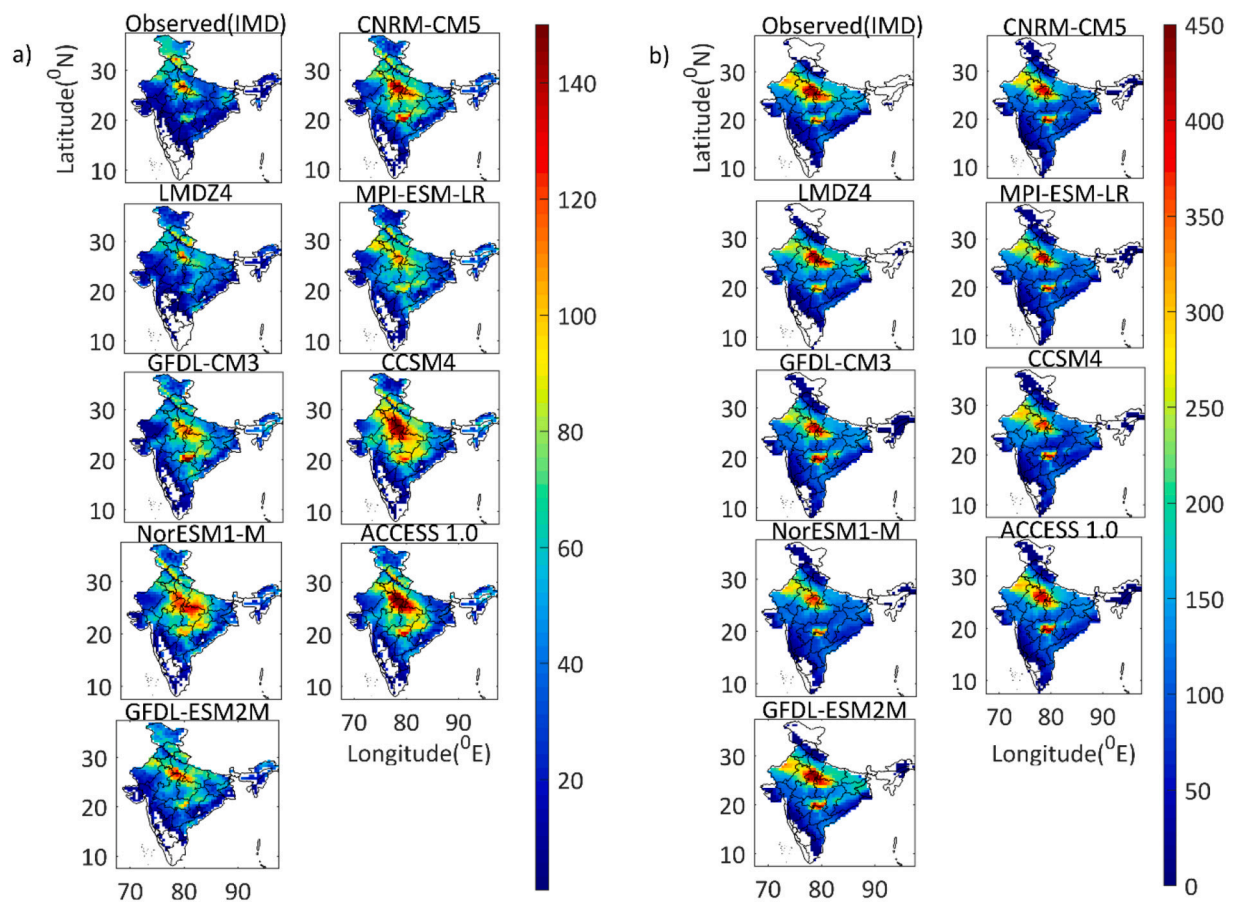
Fig. 7. Total number of observed and bias-corrected CORDEX-RCM simulated heat wave events for March–June during the period of 1971–2005 using (a) IMD and (b) IITM.

and hence are comparable. However, no heat wave is reported in northern and northeastern hilly regions according to IITM criteria (Fig. 6b) where IMD criteria observed heat wave events (Fig. 6a). Both CCAM and RegCM4 ensemble member models are able to simulate heat wave in the heat wave prone regions.

The spatial occurrence of heat wave is best simulated by LMDZ4 followed by GFDL-ESM2M according to IITM criteria while an overestimation in spatial occurrence is recorded by CCAM ensemble models in hilly areas and in the southern coastal region where heat waves being absent in observation. The LMDZ4 simulations (Fig. 7b) of heat wave

events resemble closely to observations in most of the subdivisions while GFDL-ESM2M overestimates the frequency in Vidarbha region (by around 50 events). NorESM1-M, CNRM-CM5 and GFDL-CM3 overestimate in hilly and coastal subdivisions by < 40 ± 10 events. ACCESS1.0 and CCSM4 and GFDL-CM3 simulate > 400 heat wave events over a larger spatial area in Vidarbha and Telangana sub-division which record < 350 events in observed data.
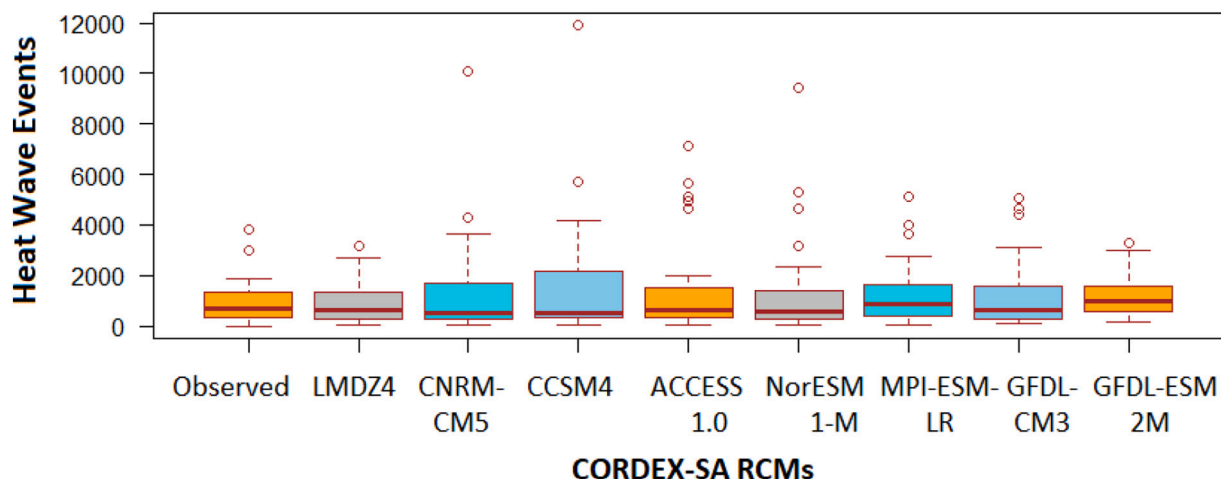

Fig. 8. Boxplots of observed and CORDEX-RCM simulated heat waves events using IMD criteria.
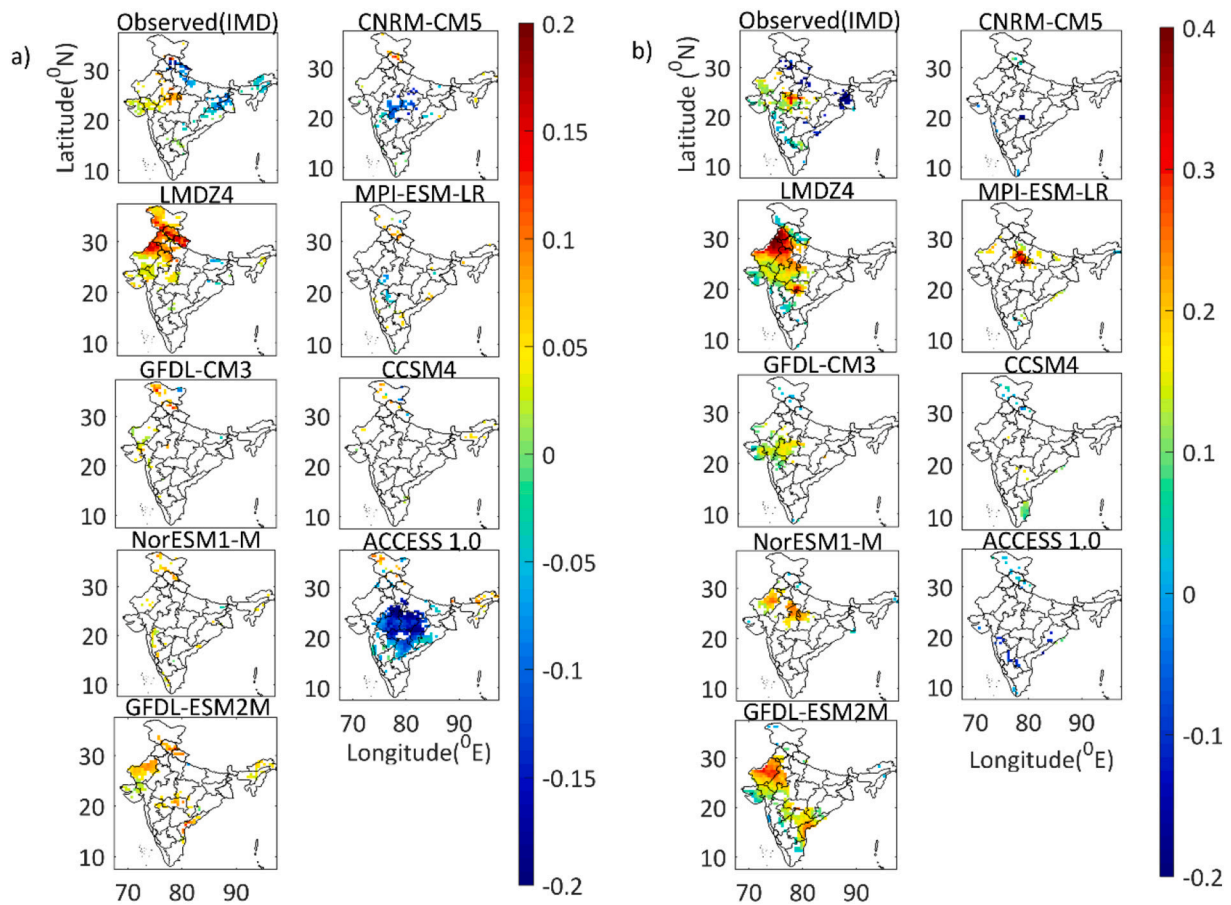
Fig. 9. Trend of observed and CORDEX-RCM simulated total number of heat wave events/year using (a) IMD criteria and (b) IITM criteria during Mar-Jun (1971–2005). The trends which are statistically significant at the 10% significance level are only shown.

3.5. Heat wave trend analysis

Student's *t*-test at 90% confidence level is conducted to estimate the trend in spatio-temporal occurrence of observed and model-simulated heat waves for each grid during Mar-Jun (1971–2005). Fig. 9. shows the spatial variability of statistically significant trend of heat wave events. For the parts of the northwestern region only LMDZ4, GFDL-ESM2M and GFDL-CM3, NorESM1-M and MPI-ESM-LR show a significant increasing trend while no significant trend is shown by other models for both IITM and IMD criteria. In which LMDZ4 overestimates the magnitude and spatial occurrence of an increasing trend 0.2 events (IMD criteria) and 0.4 events/year (IITM criteria) against the observed trend of < 0.1events/year (IMD criteria) and < 0.2 events/year (IITM criteria).

NorESM1-M also shows similar overestimation of 0.2–0.3 events/ year over the northwestern region (IITM criteria). While GFDL-ESM2M, GFDL-CM3 follow the observed trend for West Rajasthan with an increasing trend of ~0.1 events/year (IMD criteria). Overall, it was found LMDZ4 and GFDL-ESM2M are better in simulating heat waves in northwestern region. In the western region (Gujarat and Saurashtra and Kutch) only LMDZ4 and GFDL-ESM2M were found to perform well by showing a significantly increasing trend similar to the observed (< 0.1events/year) in both the criteria. GFDL-CM3 also show an increasing trend but varies in spatial occurrence and frequency which suggests the model can be improved and yield better results for the western region.

Except for CCSM4 none of the RCMs show are able to capture any of the observed negative trend of −0.1 to −0.2 events/year for the northern hilly regions. But an increasing overestimated trend of 0.05–0.2 events/year is observed by LMDZ4,GFDL-ESM2M, MPI-ESM-LR, NorESM1-M, CNRM-CM5 and GFDL-CM3 (IMD criteria) and LMDZ4 (IITM criteria) is observed. For central region (East and West MP) only LMDZ4 performs well by observing an increasing trend of 0.1–0.2 events/year according to IMD criteria while for IITM criteria significantly increasing trend is shown by LMDZ4 (0.1–0.3events/year), GFDL-ESM2M (< 0.2 events/year), GFDL-CM3 (< 0.2 events/year), NorESM1-M (0.2–0.3events/year). LMDZ4 performs well in both the criteria in the central region. Record significantly increasing trend in which the only LMDZ4 resembles closely to the observation (0.1–0.3 events/year) in both the criteria,For the south-central region (Vidarbha, Telangana, Rayalaseema) only MPI-ESM-LR show a positive increase of < 0.1 events/year (IMD) and < 0.2 events/year (IITM) as observed in few grids of Rayalaseema. While LMDZ4 overestimates increasing trend in Vidarbha and GFDL-ESM2M overestimates both in Vidarbha and Rayalaseema for IITM criteria. MPI-ESM-LR, LMDZ4 and GFDL-ESM2M can be improved and employed in studying heat wave occurrence in the south-central region.

For the eastern region, none of the models observed the declining trend of heat wave events while an overestimated increasing trend is observed in the north eastern region by CCSM4, LMDZ4, ACCESS 1.0 and GFDL-ESM2M. While CCSM4, ACCESS 1.0 and CNRM-CM5 recorded highest spatio-temporal occurrence of heat wave events, they did not show any similarity with observed in trend analysis. Overall, the results indicate that LMDZ4 and GFDL-ESM2M for RegCM411 ensemble model simulate heat wave event with better proximity to IMD observations for both the IMD and IITM criteria over India while GFDL-CM3, MPI-ESM-LR and NorESM-1 M of CCAM ensemble can be of employed to study heat waves in some regions after improvement in the models.

4. Conclusion

This study shows the importance of RCM simulated extreme temperature and confirmed the previous studies regarding the same. The analysis shows that both the RCMs were able to successfully simulate heat wave events in the northwestern, central and south-central region where the events are most pronounced according to the observation (IMD and IITM criteria). It was also found that variance scaling bias correction method removes bias and improves model simulations in capturing temperature variability. LMDZ4 and GFDL-ESM2M were found to be the best performing models in simulating heat wave frequency and spatial variability similar to observation. Whereas CCSM4 and ACCESS 1.0 overestimated heat wave frequency and spatial occurrence over India.

Long term trend analysis of heat wave events presents a different narrative of the model performance. LMDZ4 and GFDL-ESM2M showed consistency in significantly increasing trend with the observation. However, it was overestimated in some regions. CNRM-CM5, ACCESS 1.0 and CCSM4 were not able to significantly reproduce heat waves over India showing opposite trends to that of observed. Hence, they cannot be used to study heat wave characterisation and changes without improvement in them. The study also found that GFDL-CM3, NorESM1-M and MPI-ESM-LR can be further improved and explored to study heat waves over India particularly in Western, Central and South-Central region. The

Although the trend analysis did not follow the observed heat wave trend for all of the heat wave regions, the results suggest LMDZ4 and GFDL-ESM2M best performing models (RegCM4 ensemble). Thus, LMDZ4 and GFDL-ESM2M can be used for future projection studies as heat waves are strengthening with rising temperature. The study will be useful in understanding the uncertainties in CORDEX-SA RCM projections of heat wave events over India and also suggest to study different parameterisation schemes that may lead to further refinement in the representation of the land-atmosphere processes and atmospheric circulation interaction in the RCMs to capture heat waves signature well.

Availability of data and material

Authors declare that all data and materials support their published claims and comply with field standards. Authors promote data transparency and agree to provide in case of request from the journal.

Code availability

Authors declare that all software application and custom code support their published claims and comply with field standards.

Author's contribution

R K Mall conceptualize, overall supervised and provided the resources for this study. Material preparation, data collection and analysis were performed by Saumya & Jitesh. The first and final draft of the manuscript was prepared by Saumya and RKM. Sunita, JVS and A Gupta reviewed and edited the manuscript at different stages. All authors read and approved the final manuscript.

Declaration of Competing Interest

The authors declare that they have no known competing financial interests or personal relationships that could have appeared to influence the work reported in this paper.

Appendix A. Supplementary data

Supplementary data to this article can be found online at https:// doi.org/10.1016/j.atmosres.2020.105228.

References

Alexander, L.V., Arblaster, J.M., 2017. Historical and projected trends in temperature and precipitation extremes in Australia in observations and CMIP5. Weather Clim. Extrem. 15, 34–56. https://doi.org/10.1016/j.wace.2017.02.001.

Alexander, L.V., Allen, S.K., Breon, F.-M., Church, J.A., 2013. IPCC AR5. Summary for Policymakers. https://doi.org/10.1017/CBO9781107415324.004.

Alias, A., et al., 2017. Future summer mega-heatwave and record-breaking temperatures in a warmer France climate. Environ. Res. Lett. 12, 074025. https://doi.org/10.1088/1748-9326/aa751c.

Almagro, A., Oliveira, P.T.S., Rosolem, R., Hagemann, S., Nobre, C.A., 2020. Performance evaluation of Eta/HadGEM2-ES and Eta/MIROC5 precipitation simulations over Brazil. Atmos. Res. 244, 105053. https://doi.org/10.1016/j.atmosres.2020.105053.

Attri, S.D., Tyagi, A., 2010. Climate profile of India. Environ. Meteorol. India Meteorol. Dep. 1–122. https://doi.org/10.1007/s12524-010-0015-9.

Baldwin, J.W., Dessy, J.B., Vecchi, G.A., Oppenheimer, M., 2019. Temporally compound Heat Wave events and Global Warming: an Emerging Hazard. Earth's Futur. 7, 411–427. https://doi.org/10.1029/2018EF000989.

Basu, R., 2009. High ambient temperature and mortality: a review of epidemiologic studies from 2001 to 2008. Environ. Heal. A Glob. Access Sci. Source 8. https://doi.org/10.1186/1476-069X-8-40.

Bentsen, M., Bethke, I., Debernard, J.B., Iversen, T., Kirkevåg, A., Seland, Ø., Drange, H., Roelandt, C., Seierstad, I.A., Hoose, C., Kristjánsson, J.E., 2013. The Norwegian Earth System Model, NorESM1-M – Part 1: Description and basic evaluation of the physical climate. Geosci. Model Dev. 6, 687–720. https://doi.org/10.5194/gmd-6-687-2013.

Bi, D., Dix, et al., 2013. The ACCESS coupled model: description, control climate and preliminary validation. Aust. Meteorol. Oceanogr. J. 63, 41–64. https://doi.org/10.22499/2.6301.004.

Chen, J., Brissette, F.P., Leconte, R., 2011a. Uncertainty of downscaling method in quantifying the impact of climate change on hydrology. J. Hydrol. 401 (3–4), 190–202. https://doi.org/10.1016/j.jhydrol.2011.02.020.

Chen, J., Brissette, F.P., Poulin, A., Leconte, R., 2011b. Overall uncertainty study of the hydrological impacts of climate change for a Canadian watershed. Water Resour. Res. 47, 1–16. https://doi.org/10.1029/2011WR010602.

Chen, J., Brissette, F.P., Chaumont, D., Braun, M., 2013. Finding appropriate bias correction methods in downscaling precipitation for hydrologic impact studies over North America. Water Resour. Res. 49, 4187–4205. https://doi.org/10.1002/wrcr.20331.

Choudhary, A., Dimri, A.P., Maharana, P., 2018. Assessment of CORDEX-SA experiments in representing precipitation climatology of summer monsoon over India. Theor. Appl. Climatol. 134, 283–307. https://doi.org/10.1007/s00704-017-2274-7.

Christensen, J.H., Boberg, F., Christensen, O.B., Lucas-Picher, P., 2008. On the need for bias correction of regional climate change projections of temperature and precipitation. Geophys. Res. Lett. 35. https://doi.org/10.1029/2008GL035694.

Collier, M., Uhe, P., 2012. CMIP5 datasets from the ACCESS1.0 and ACCESS1.3 coupled climate models. CAWCR Tech. Rep 059. 20978-1-922173-29-4.

Dunne, J.P., John, J.G., Adcroft, A.J., Griffies, S.M., Hallberg, R.W., Shevliakova, E., Stouffer, R.J., Cooke, W., Dunne, K.A., Harrison, M.J., Krasting, J.P., Malyshev, S.L., Milly, P.C.D., Phillipps, P.J., Sentman, L.T., Samuels, B.L., Spelman, M.J., Winton, M., Wittenberg, A.T., Zadeh, N., 2012. GFDL's ESM2 global coupled climate-carbon earth system models. Part I: Physical formulation and baseline simulation characteristics. J. Clim. 25, 6646–6665. https://doi.org/10.1175/JCLI-D-11-00560.1.

Fang, G.H., Yang, J., Chen, Y.N., Zammit, C., 2015. Comparing Bias Correction Methods in Downscaling Meteorological Variables for a Hydrologic Impact Study in an Arid Area in China. Hydrol. Earth Syst. Sci. 19, 2547–2559. https://doi.org/10.5194/hess-

19-2547-2015.

García, F.C., Bestiona, E., Warfielda, R., Yvon-Durochera, G., 2018. Changes in temperature alter the relationship between biodiversity and ecosystem functioning. Proc. Natl. Acad. Sci. U. S. A. 115, 10989–10994. https://doi.org/10.1073/pnas. 1805518115.

Gent, P.R., Danabasoglu, G., Donner, L.J., Holland, M.M., Hunke, E.C., Jayne, S.R., Lawrence, D.M., Neale, R.B., Rasch, P.J., Vertenstein, M., Worley, P.H., Yang, Z.L., Zhang, M., 2011. The community climate system model version 4. J. Clim. 24, 4973–4991. https://doi.org/10.1175/2011JCLI4083.1.

Ghatak, D., Zaitchik, B., Hain, C., Anderson, M., 2017. The role of local heating in the 2015 Indian Heat Wave. Sci. Rep. 7, 1–8. https://doi.org/10.1038/s41598-017-07956-5.

Giorgetta, M.A., et al., 2013. Climate and carbon cycle changes from 1850 to 2100 in MPI-ESM simulations for the coupled Model Intercomparison Project phase 5. J. Adv. Model. Earth Syst. 5, 572–597. https://doi.org/10.1002/jame.20038.

Giorgi, F., Jones, C., Asrar, G., 2009. Addressing climate information needs at the regional level: the CORDEX framework. Organ. Bull. 58, 175–183.

Giorgi, F., Coppola, E., Solmon, F., Mariotti, L., Sylla, M.B., Bi, X., Elguindi, N., Diro, G.T., Nair, V., Giuliani, G., Turuncoglu, U.U., Cozzini, S., Güttler, I., O'Brien, T.A., Tawfik, A.B., Shalaby, A., Zakey, A.S., Steiner, A.L., Stordal, F., Sloan, L.C., Brankovic, C., 2012. RegCM4: Model description and preliminary tests over multiple CORDEX domains. Clim. Res. 52, 7–29. https://doi.org/10.3354/cr01018.

Gleckler, P.J., Taylor, K.E., Doutriaux, C., 2008. Performance metrics for climate models. J. Geophys. Res. Atmos. 113, 1–20. https://doi.org/10.1029/2007JD008972.

Gosling, S.N., Lowe, J.A., McGregor, G.R., Pelling, M., Malamud, B.D., 2009. Associations between elevated atmospheric temperature and human mortality: a critical review of the literature. Clim. Chang. 92, 299–341. https://doi.org/10.1007/s10584-008-9441-x.

Griffies, S.M., Winton, M., Donner, L.J., Horowitz, L.W., Downes, S.M., Farneti, R., Gnanadesikan, A., Hurlin, W.J., Lee, H.C., Liang, Z., Palter, J.B., Samuels, B.L., Wittenberg, A.T., Wyman, B.L., Yin, J., Zadeh, N., 2011. The GFDL CM3 coupled climate model: Characteristics of the ocean and sea ice simulations. J. Clim. 24, 3520–3544. https://doi.org/10.1175/2011JCLI3964.1.

Gupta, P., Verma, S., Bhatla, R., Chandel, A.S., Singh, Payra, S., 2020. Validation of surface temperature derived from MERRA-2 Reanalysis against IMD gridded data set over India. Earth and Space Science 7https://doi.org/10.1029/2019EA000910. e2019EA000910.

Harrison, S.P., Bartlein, P.J., Izumi, K., Li, G., Annan, J., Hargreaves, J., Braconnot, P., Kageyama, M., 2015. Evaluation of CMIP5 palaeo-simulations to improve climate projections. Nat. Clim. Chang. 5, 735–743. https://doi.org/10.1038/nclimate2649.

IPCC, 2013. The physical science basis. Contribution of Working Group I to the Fifth Assessment Report of the Intergovernmental Panel on Climate Change. Cambridge University Press, United Kingdom and New York, USA. https://doi.org/10.1017/CBO9781107415324.024.

IMD, 2018. Earth System Science Organization (ESSO) Ministry of Earth Sciences (MoES), India, Heat wave bulletein. All India Heat Wave Information, 5. Accessed 8 August 2018.

Jacob, D., Petersen, J., Eggert, B., Alias, A., Christensen, O.B., Bouwer, L.M., Braun, A., Colette, A., Déqué, M., Georgievski, G., Georgopoulou, E., Gobiet, A., Menut, L., Nikulin, G., Haensler, A., Hempelmann, N., Jones, C., Keuler, K., Kovats, S., Kröner, N., Kotlarski, S., Kriegsmann, A., Martin, E., van Meijgaard, E., Moseley, C., Pfeifer, S., Preuschmann, S., Radermacher, C., Radtke, K., Rechid, D., Rounsevell, M., Samuelsson, P., Somot, S., Soussana, J.F., Teichmann, C., Valentini, R., Vautard, R., Weber, B., Yiou, P., 2014. EURO-CORDEX: New high-resolution climate change projections for European impact research. Reg. Environ. Chang. 14, 563–578. https://doi.org/10.1007/s10113-013-0499-2.

Karl, T., Nicholls, N., Ghazi, A., 1999. Workshop on Indices and Indicators for climate Extremes Precipitation.Pdf. Clim. Chang. 42, 3–7. https://doi.org/10.1007/978-94-015-9265-9-2.

Krishnan, R., Sanjay, J., Gnanaseelan, C., Mujumdar, M., Kulkarni, A., Chakraborty, S., 2020. Assessment of Climate Change over the Indian Region: A Report of the Ministry of Earth Sciences (MoES), Government of India. pp. 226. https://doi.org/10.1007/978-981-15-4327-2.

Lhotka, O., Kyselý, J., Plavcová, E., 2017. Evaluation of major heat waves ' mechanisms in EURO-CORDEX RCMs over Central Europe. Clim. Dyn. 50, 4249–4262. https://doi.org/10.1007/s00382-017-3873-9.

Mall, R.K., Sonkar, G., Bhatt, D., Sharma, N.K., Baxla, A.K., Singh, K.K., 2016. Managing impact of extreme weather events in sugarcane in different agro-climatic zones of Uttar Pradesh. Mausam 67, 233–250.

Mall, R.K., Singh, N., Singh, K.K., Sonkar, G., Gupta, A., 2018. Evaluating the performance of RegCM4. 0 climate model for climate change impact assessment on wheat and rice crop in diverse agro-climatic zones of Uttar Pradesh, India. Clim. Chang. 149 (3–4), 503–515.

Mall, R.K., Srivastava, R.K., Banerjee, T., Mishra, O.P., Bhatt, D., Sonkar, G., 2019. Disaster risk reduction including climate change adaptation over South Asia: challenges and ways forward. Int. J. Disaster Risk Sci. 10 (1), 14–27. https://doi.org/10.1007/s13753-018-0210-9.

Mandal, R., Joseph, S., Sahai, A.K., Phani, R., Dey, A., Chattopadhyay, R., 2019. Real time extended range prediction of heat waves over India. Sci. Rep. 1–11. https://doi.org/10.1038/s41598-019-45430-6.

Mcgregor, J.L., Dix, M.R., 2001. The CSIRO Conformal-Cubic Atmospheric GCM. In: Hodnett, P F (Ed.), IUTAM Symposium on Advances in Mathematical Modelling of Atmosphere and Ocean Dynamics. Fluid Mechanics and Its Applications. 61 Springer, Dordrecht. https://doi.org/10.1007/978-94-010-0792-4_25.

Meehl, G.A., Covey, C., Delworth, T., Latif, M., McAvaney, B., Mitchell, J.F.B., Stouffer, R.J., Taylor, K.E., 2007. The WCRP CMIP3 multimodel dataset: a new era in climatic

change research. Bull. Am. Meteorol. Soc. 88, 1383–1394. https://doi.org/10.1175/BAMS-88-9-1383.

Miao, C., Duan, Q., Sun, Q., Huang, Y., Kong, D., Yang, T., Ye, A., Di, Z., Gong, W., 2014. Assessment of CMIP5 climate models and projected temperature changes over Northern Eurasia. Environ. Res. Lett. 9. https://doi.org/10.1088/1748-9326/9/5/055007.

Mishra, V., Mukherjee, S., Kumar, R., Stone, D.A., 2017b. Heat wave exposure in India in current, 1.5 °c, and 2.0 °c worlds. Environ. Res. Lett. 12. https://doi.org/10.1088/1748-9326/aa9388.

Mukherjee, S., Mishra, V., 2018. Concurrent day and nighttime heatwaves in India under 1.5, 2.0, and 3.0°C warming world. pp. 1–9. https://doi.org/10.1038/s41598-018-35348-w.

Murari, K.K., Ghosh, S., Patwardhan, A., Daly, E., Salvi, K., 2015. Intensification of future severe heat waves in India and their effect on heat stress and mortality. Reg. Environ. Chang. 15, 569–579. https://doi.org/10.1007/s10113-014-0660-6.

Nayak, S., Mandal, M., Maity, S., 2019. Performance evaluation of RegCM4 in simulating temperature and precipitation climatology over India. Theor. Appl. Climatol. 137, 1059–1075. https://doi.org/10.1007/s00704-018-2635-x.

Obradovich, N., Migliorini, R., Paulus, M.P., Rahwan, I., 2018. Empirical evidence of mental health risks posed by climate change. Proc. Natl. Acad. Sci. U. S. A. 115, 10953–10958. https://doi.org/10.1073/pnas.1801528115.

O'Brien, T.A., Kashinath, K., Cavanaugh, N.R., Collins, W.D., O'Brien, J.P., 2016. A fast and objective multidimensional kernel density estimation method: FastKDE. Comput. Stat. Data Anal. 101, 148–160. https://doi.org/10.1016/j.csda.2016.02.014.

Pai, D.S., Nair, S.A., Ramanathan, A.N., 2013. Long term climatology and trends of heat waves over India during the recent 50 years (1961-2010). Mausam 64, 585–604.

Panda, D.K., AghaKouchak, A., Ambast, S.K., 2017. Increasing heat waves and warm spells in India, observed from a multiaspect framework. J. Geophys. Res. 122, 3837–3858. https://doi.org/10.1002/2016JD026292.

Panjwani, S., Naresh Kumar, S., Ahuja, L., Islam, A., 2020. Evaluation of selected global climate models for extreme temperature events over India. Theor. Appl. Climatol. 140, 731–738. https://doi.org/10.1007/s00704-020-03108-4.

Pattnayak, K.C., Panda, S.K., Saraswat, V., Dash, S.K., 2018. Assessment of two versions of regional climate model in simulating the Indian Summer Monsoon over South Asia CORDEX domain. Clim. Dyn. 50, 3049–3061. https://doi.org/10.1007/s00382-017-3792-9.

de Perez, E.C., Mason, S., van Aalst, M., Stephens, E., van den Hurk, B., Bischiniotis, K., Zsoter, E., Nissan, H., Pappenberger, F., 2018. Global predictability of temperature extremes. Environ. Res. Lett. 13, 054017. https://doi.org/10.1088/1748-9326/aab94a.

Perkins, S.E., 2015. A review on the scientific understanding of heatwaves-their measurement, driving mechanisms, and changes at the global scale. Atmos. Res. 164–165, 242–267. https://doi.org/10.1016/j.atmosres.2015.05.014.

Perkins, S.E., Alexander, L.V., 2012. AMS Journals Online - on the Measurement of Heat Waves. J. Clim. 4500–4517. https://doi.org/10.1175/JCLI-D-12-00383.1.

Perkins-Kirkpatrick, S.E., Gibson, P.B., 2017. Changes in regional heatwave characteristics as a function of increasing global temperature. Sci. Rep. 7, 1–12. https://doi.org/10.1038/s41598-017-12520-2.

Peterson, T.C., Folland, C.C., Gruza, G., Hogg, W., Mokssit, A., Plummer, N., 2001. Report on the activities of the working group on climate change detection and related rapporteurs 1998–2001. Rep. WCDMP-47, WMO-TD 1071 143. https://doi.org/WMO, Rep. WCDMP-47,WMO-TD 1071.

Prajapat, D.K., Lodha, J., Choudhary, M., 2020. A spatiotemporal analysis of Indian warming target using CORDEX-SA experiment data. Theor. Appl. Climatol. 139, 447–459. https://doi.org/10.1007/s00704-019-02978-7.

Purich, A., Sadler, K., Pezza, A., Boschat, G., Cowan, T., Perkins, S., 2014. More frequent, longer, and Hotter Heat Waves for Australia in the Twenty-first Century. J. Clim. 27, 5851–5871. https://doi.org/10.1175/jcli-d-14-00092.1.

Quesada, B., Vautard, R., Yiou, P., Hirschi, M., Seneviratne, S.I., 2012. Asymmetric European summer heat predictability from wet and dry southern winters and springs. Nat. Clim. Chang. 2, 736–741. https://doi.org/10.1038/nclimate1536.

Racherla, P.N., Shindell, D.T., Faluvegi, G.S., 2012. The added value to global model projections of climate change by dynamical downscaling: a case study over the continental U.S. using the GISS-ModelE2 and WRF models. J. Geophys. Res. Atmos. 117, 8–15. https://doi.org/10.1029/2012JD018091.

Ratnam, J.V., Behera, S.K., Ratna, S.B., Rajeevan, M., Yamagata, T., 2016. Anatomy of Indian heatwaves. Sci. Rep. 6, 1–11. https://doi.org/10.1038/srep24395.

Rohini, P., Rajeevan, M., Srivastava, A.K., 2016. On the Variability and increasing Trends of Heat Waves over India. Sci. Rep. 6, 1–9. https://doi.org/10.1038/srep26153.

Rohini, P., Rajeevan, M., Mukhopadhay, P., 2019. Future projections of heat waves over India from CMIP5 models. Clim. Dyn. 53, 975–988. https://doi.org/10.1007/s00382-019-04700-9.

Russo, S., Dosio, A., Graversen, R.G., Sillmann, J., Carrao, H., Dunbar, M.B., Singleton, A., Montagna, P., Barbola, P., Vogt, J.V., 2014. Magnitude of extreme heat waves in present climate and their projection in a warming world. J. Geophys. Res. Atmos. 119, 12500–12512. https://doi.org/10.1002/2014JD022098.

Russo, S., Sillmann, J., Fischer, E.M., 2015. Top ten European heatwaves since 1950 and their occur- rence in the future. Environ. Res. Lett. 10, 124003. https://doi.org/10.1088/1748-9326/10/12/124003.

Sabin, T.P., Krishnan, R., Ghattas, J., Denvil, S., Dufresne, J.L., Hourdin, F., Pascal, T., 2013. High-resolution simulation of the south Asian monsoon using a variable resolution global climate model. Clim. Dyn. 41, 173–194. https://doi.org/10.1007/s00382-012-1658-8.

Sanjay, J., Krishnan, R., Bhakta, A., 2017. ScienceDirect Downscaled climate change projections for the Hindu Kush Himalayan region using CORDEX South Asia regional climate models. Adv. Clim. Chang. Res. 8, 185–198. https://doi.org/10.1016/j.accre.

2017.08.003.

Schmidli, J., Frei, C., Vidale, P.L., 2006. Downscaling from GCM precipitation: a benchmark for dynamical and statistical downscaling methods. Int. J. Climatol. 26, 679–689. https://doi.org/10.1002/joc.1287.

Sharma, S., Mujumdar, P., 2017. 'Increasing frequency and spatial extent of concurrent meteorological droughts and heatwaves in India', Sci. Rep. 7 (1), 1–9. https://doi.org/10.1038/s41598-017-15896-3.

Sillmann, J., Kharin, V.V., Zhang, X., Zwiers, F.W., Bronaugh, D., 2013. Climate extremes indices in the CMIP5 multimodel ensemble: part 1. Model evaluation in the present climate. J. Geophys. Res. Atmos. 118, 1716–1733. https://doi.org/10.1002/jgrd.50203.

Singh, N., Mhawish, A., Ghosh, S., Banerjee, T., Mall, R.K., 2019. Attributing mortality from temperature extremes: a time series analysis in Varanasi, India. Sci. Total Environ. 665, 453–464. https://doi.org/10.1016/j.scitotenv.2019.02.074.

Singh, N., Singh, S., Mall, R.K., 2020. Urban ecology and human health: implications of urban heat island, air pollution and climate change nexus. In: Verma, P., Singh, P.A., Singh, R., Raghubanshi, A.S. (Eds.), Urban Ecology. Elsevier, pp. 317–334. https://doi.org/10.1016/B978-0-12-820730-7.00017-3.

Sonkar, G., Mall, R.K., Banerjee, T., Singh, N., Kumar, T.L., Chand, R., 2019. Vulnerability of Indian wheat against rising temperature and aerosols. Environ. Pollut. 254, 112946. https://doi.org/10.1016/j.envpol.2019.07.114.

Sonkar, G., Singh, N., Mall, R.K., Singh, K.K., Gupta, A., 2020. 2020. Simulating the Impacts of climate Change on Sugarcane in Diverse Agro-climatic zones of Northern India using CANEGRO-Sugarcane Model. Sugar Tech 22, 460–472. https://doi.org/10.1007/s12355-019-00787-w.

Srivastava, A., Rajeevan, M., Kshirsagar, S., 2009. Development of a high-resolution daily gridded temperature data set (1969–2005) for the Indian region. Atmos. Sci. Lett. 10, 249–254. https://doi.org/10.1002/asl.

Tang, J., Niu, X., Wang, S., Gao, H., Wang, X., Wu, J., 2016. Statistical downscaling and dynamical downscaling of regional climate in China: present climate evaluations and future climate projections. J. Geophys. Res. 121, 2110–2129. https://doi.org/10.1002/2015JD023977.

Taylor, K.E., 2001. In a Single Diagram. J. Geophys. Res. 106, 7183–7192. https://doi.org/10.1029/2000JD900719.

Taylor, K.E., Stouffer, R.J., Meehl, G.A., 2012. An overview of CMIP5 and the experiment design. Bull. Am. Meteorol. Soc. 93 (4), 485–498.

Teutschbein, C., Seibert, J., 2012. Bias correction of regional climate model simulations for hydrological climate-change impact studies: Review and evaluation of different methods. J. Hydrol. 456–457, 12–29. https://doi.org/10.1016/j.jhydrol.2012.05.052.

Themeßl, M.J., Gobiet, A., Heinrich, G., 2012. Empirical-statistical downscaling and error correction of regional climate models and its impact on the climate change signal. Clim. Chang. 112, 449–468. https://doi.org/10.1007/s10584-011-0224-4.

Vautard, R., Gobiet, A., Jacob, D., Belda, M., Colette, A., Déqué, M., Fernández, J., García-Díez, M., Goergen, K., Güttler, I., Halenka, T., Karacostas, T., Katragkou, E., Keuler, K., Kotlarski, S., Mayer, S., van Meijgaard, E., Nikulin, G., Patarčić, M., Scinocca, J., Sobolowski, S., Suklitsch, M., Teichmann, C., Warrach-Sagi, K., Wulfmeyer, V., Yiou, P., 2013. The simulation of European heat waves from an ensemble of regional climate models within the EURO-CORDEX project. Clim. Dyn. 41, 2555–2575. https://doi.org/10.1007/s00382-013-1714-z.

Vogel, E., Donat, M.G., Alexander, L.V., Meinshausen, M., Ray, D.K., Karoly, D., Meinshausen, N., Frieler, K., 2019. The effects of climate extremes on global agricultural yields. Environ. Res. Lett. 14 (5), 054010.

Voldoire, A., Sanchez-Gomez, E., Salas y Mélia, D., Decharme, B., Cassou, C., Sénési, S., Valcke, S., Beau, I., Alias, A., Chevallier, M., Déqué, M., Deshayes, J., Douville, H., Fernandez, E., Madec, G., Maisonnave, E., Moine, M.P., Planton, S., Saint-Martin, D., Szopa, S., Tyteca, S., Alkama, R., Belamari, S., Braun, A., Coquart, L., Chauvin, F., 2013. The CNRM-CM5.1 global climate model: Description and basic evaluation. Clim. Dyn. 40, 2091–2121. https://doi.org/10.1007/s00382-011-1259-y.

Wang, L., Ranasinghe, R., Maskey, S., van Gelder, P.H.A.J.M., Vrijling, J.K., 2016. Comparison of empirical statistical methods for downscaling daily climate projections from CMIP5 GCMs: a case study of the Huai River Basin. China. Int. J. Climatol. 36, 145–164. https://doi.org/10.1002/joc.4334.

Willmott, C.J., 1981. On the Validation of Models. Phys. Geogr. 2 (2), 184–194. https://doi.org/10.1080/02723646.1981.10642213.

Xu, Z., Han, Y., Yang, Z., 2019. Dynamical downscaling of regional climate: a review of methods and limitations. Sci. China Earth Sci. 62, 365–375. https://doi.org/10.1007/s11430-018-9261-5.

Yao, Y., Yong, L., Jian-Bin, H., 2013. Evaluation and projection of temperature extremes over China based on CMIP5 model. Adv. Clim. Chang. Res. 3, 179–185. https://doi.org/10.3724/sp.j.1248.2012.00179.